Research Journal of Recent Sciences E-ISSN 2277-2502
Vol. **5(2),** 56-65, February **(2016)** *Res.J.Recent Sci.*

Torque Comparison between a Novel Multilayer Switched Reluctance Motor and a Custom one

Alireza Siadatan[1*], Mohammad Mahdi Mahmoodi[2] and Mohammad Mehdi Nezamabadi[1]
[1]Department of Electrical Engineering, West Tehran Branch, Islamic Azad University, Tehran, Iran
[2]Department of Electrical Engineering, Saveh Branch, Islamic Azad University, Saveh, Iran
a_siadatan@wtiau.ac.ir

Available online at: www.isca.in, www.isca.me
Received 15th January 2014, revised 22nd February 2015, accepted 18th October 2015

Abstract

In this paper a custom three phase Switched Reluctance Motor (SRM) with six stator and four rotor salient poles (6 by 4) was designed, simulated and analyzed and it's produced torque, phase inductance, flux linkage and some other characteristics were obtained by the 3D Finite Element Method (FEM). Then a novel 7-layer 4 by 4 Multilayer SRM (MSRM) with the same volume was designed and under the same conditions was simulated and analyzed. In the latter motor, 3 layers are energized at the same time causing more torque and efficiency and less torque ripple. Both motors were analyzed under different situations and results were attained. Finally prototypes of each one in the laboratory were constructed and tested and the results were compared with the simulations.

Keywords: Torque, MSRM, FEM.

Introduction

The SRM is one of the special motor for low cost and simple structure in variable speed drive applications such as cars, home appliances, and industrial[1,2]. Many types of SRMs are presented. The general classification of SRMs is illustrated in Figure-1. There are two types of SRMs. Linear SRM and the rotary SRM. The linear SRM is divided in single stack SRM and multi stack SRM. Rotary SRM has two types of radial field and axial field SRM. In some radial field SRM the rotor is the outer part and the stator is the inner part. In some others the rotor is rotated inside the stator. The axial field SRM has two types of multi stack with internal rotor and single stack with external rotor[3,4].

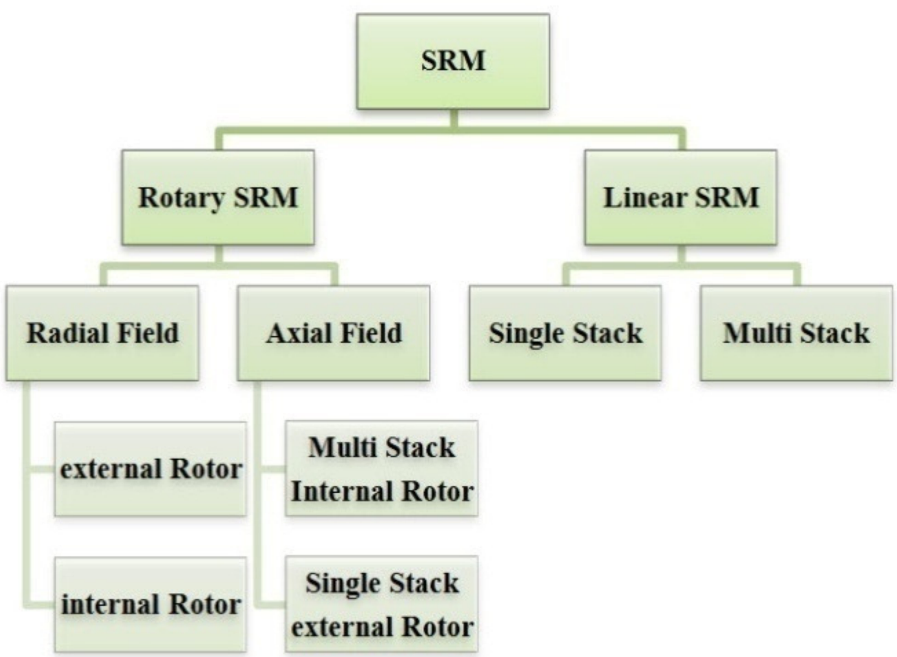

Figure-1
SRM general types

Various configurations of this machine are proposed in the literatures with specific characteristics, such as; isolated double layer[5], dual channel[6], hybrid stator pole[7], linear[8,9], multi-layer[10], and disc-type[11] machine. C. Lee and R. Krishnan introduced a two-phase SRM using common pole E-core structure which its stator has four small poles and two or four large poles between small poles. Its common poles do not have copper windings and are shared by both phases for positive torque production through the entire operation[12]. Two new two-phase SRM with modified rotor poles shape and optimized torque have been presented[13]. Different geometries have been proposed by S. G. Oh, and R. Krishnan with six stator and three rotor poles[14]. They are designed with different pole arcs and some with variable air gaps. A new hybrid Switched Reluctance Motor/Generator (SRMG) with salient stator pole was introduced after which it has a pair of permanent magnets attached symmetrically between the iron poles of the rotor[15]. H. Chen and J. J. Gu presented a three-phase SRMG. One is a dual motors drive for the electric locomotive traction; the other is a variable-speed generator system for wind power applications[16]. The operating characteristics of the SRG excited by a Suppression Resistor Converter (SRC) based on FEM analysis and experiments are examined[17]. N. Radimov considered the operation of the SRMG as an autonomous three-phase AC generator[18]. The generator circuit consists of only capacitors and load supplementary to the generator, but does not contain any power supply. M. S. Toulabi et. al. suggested a new hybrid two-phase SRMG which consists of two independent stator and rotor sets where each stator pole has 45º arc length. Each rotor pole is the same as stator pole (45º) in one side and twice as much in the other side[19].

MSRMs are new SRMs with more than one independent layer. Their advantages especially the improvement in torque per volume parameter makes them so attractive to enter industry. A new three-layer MSRM with eight stator salient poles and 6 rotor salient poles is introduced by Afjei and Toliyat[20].

This paper presents the characteristics and comparison of two types of SRMs which are 6 by 4 conventional SRM and a 7-layer 4 by 4 MSRM. These motors have the same iron volume.

In section II, the specifications of the 6 by 4 SRM is explained. In section III the specifications of 7-layer MSRM are presented. In section IV, these motors are simulated and different parameters of them are obtained by 3D FEM and the simulation results are compared to each other. In section V, the motors are constructed and the operational results of them are compared to each other. The paper is finished by conclusion in section VI.

The Conventional 6 By 4 Srm Specifications

The conventional 6 by 4 SRM has six stator and four rotor salient poles. The motor shape is shown in Figure 2. The arc of the stator pole is 29 degree and the arc of the rotor pole is 32 degrees. The motor specifications are presented in table 1. The stator and rotor poles are made up of M-27 laminations of non-oriented silicon steel whose static B-H curve is shown in Figure 3. The 6 by 4 SRM proto type is fabricated in laboratory which is shown in Figure-4.

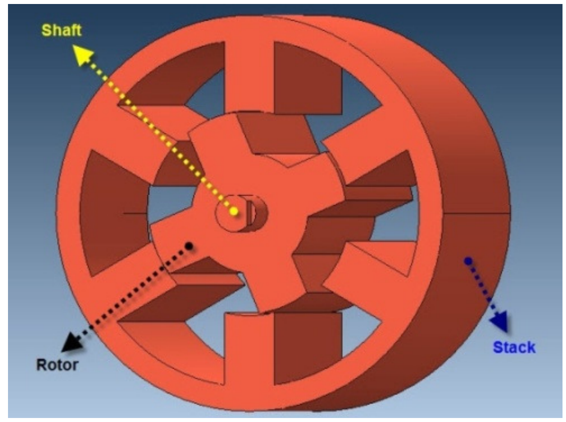

Figure-2
6 by 4 SRM

Table-1
The Specifications of the 6 by 4 three-phase SRM

Nominal Power	1hp
Nominal voltage	60 V
Nominal speed	3000 rpm
Stack length	175 mm
Stator outer diameter	182.1mm
Stator inner diameter	148.7mm
Stator pole arc	29°
Rotor outer diameter	148.4mm
Rotor shaft diameter	20mm
Rotor pole arc	31°
Air gap between stator and rotor pole	0.25mm
Number of winding turns per pole	80 turns
Each phase resistance	1.5 Ω

Seven-Layer 4 By 4 Msrm Specifications

The 7-layer 4 by 4 MSRM includes four independent stator and rotor salient poles in each layer. The windings of stator poles in each layer are in series making up a phase. So this type of motor has the advantages of the less maintenance requirement, having no isolation problem, producing more torque with less torque ripple and working smoother.

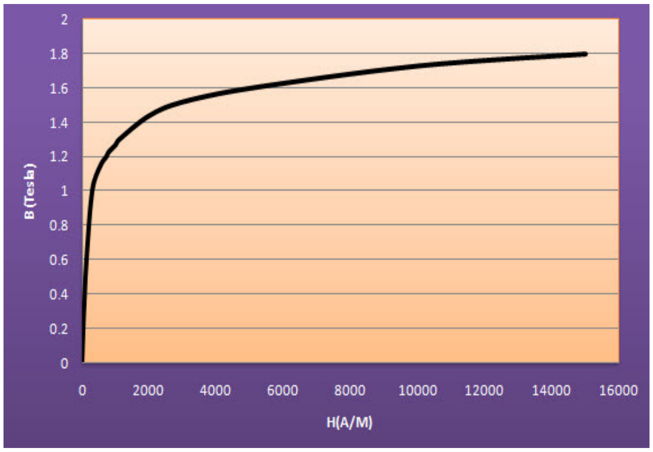

Figure-3
B-H curve of the used M-27 laminations

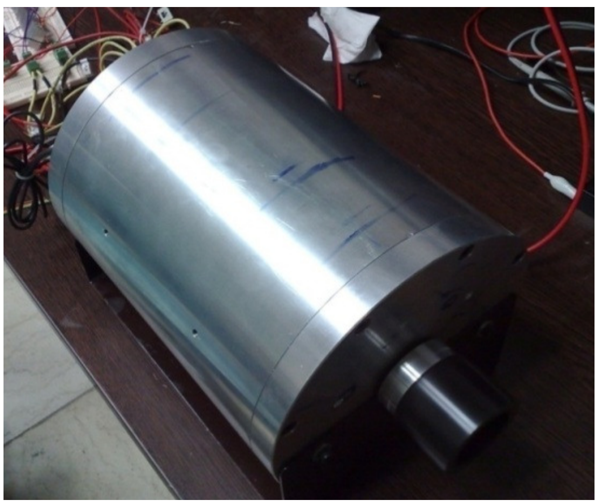

Figure-4
The fabricated 6 by 4 SRM

The Rotor of each layer is shifted some degrees in comparison to other layers which is calculated by Equation-1:

$$\theta_{\text{shift}_{7-\text{Layer}}} = \frac{\frac{360}{\text{number of poles in Stator}}}{\text{Number of Layers in MSRM}} = \frac{\frac{360}{4}}{7} = 12.85^\circ \quad (1)$$

The motor shape is shown in Figure-5. The arc of the stator pole is 44 degree and the arc of the rotor pole is 46 degrees. The specifications of this type of MSRM are presented in Table-2. The stator and rotor poles are made up of M-27 lamination of non-oriented silicon steel just like other presented SRMs. The 7-layer 4 by 4 MSRM proto type is also built in laboratory and illustrated in Figure-6.

This type of motor is also designed in a way that a number of layers (phases) can be switched on at the same time. In this MSRM three layers are switched on each time. The phase switching algorithm of the 7-layer MSRM is presented in Table-3.

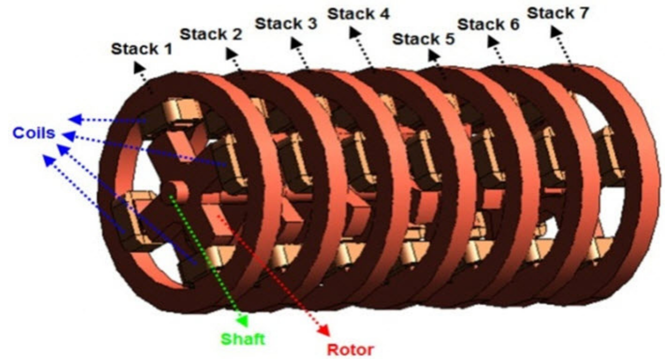

Figure-5
7-layer 4 by 4 MSRM in magnet

Table-2
The specification of the 7-layer 4 by 4 MSRM

Nominal Power	1hp
Nominal voltage	60 V
Nominal speed	3000 rpm
Each layer Stack length	25 mm
Stator outer diameter	182.1mm
Stator inner diameter	148.7mm
Stator pole arc	44°
Rotor outer diameter	148.4mm
Rotor shaft diameter	20mm
Rotor pole arc	46°
Air gap between stator and rotor pole	0.25mm
Number of winding turns per pole	100 turns
Each phase resistance	1.1 Ω

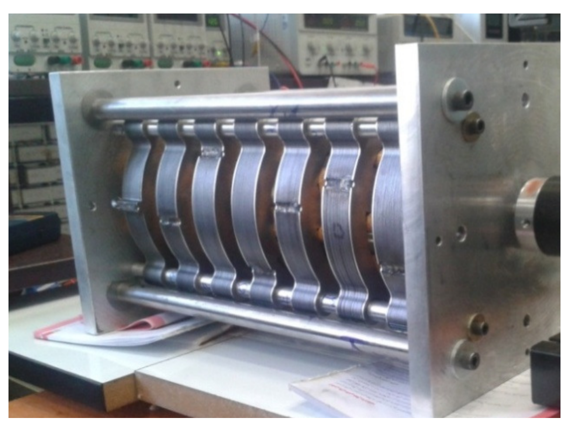

Figure-6
The fabricated 7-layer 4 by 4 MSRM

Table-3
The phase switching algorithm in the 7-layer MSRM

	Ph1	**Ph2**	**Ph3**	**Ph4**	**Ph5**	**Ph6**	**Ph7**
C1	On	On	On	off	off	off	off
C2	off	On	On	On	off	off	off
C3	off	off	On	On	On	off	off
C4	off	off	off	On	On	On	off
C5	off	off	off	off	On	On	On
C6	On	off	off	off	off	On	On
C7	On	On	off	off	off	off	On
CX = Case X PhX = Phase X							

The Presented Motors Analyses By 3d Fem

After motor designing, it should be simulated in order to obtain an accurate model of the motor. Different parameters of motors are obtained during simulations which are so important. The presented motors in this paper are simulated in Magnet Infolytica Package in which 3D FEM is used[21]. Magnet can also simulate the two dimensional model but 3D simulation results are more accurate although it requires more time. To obtain the different parameters of SRM, the motor phase is exited in different positions of rotor. Electric vector potential (T) is used solve the problems which is calculated by:

$$J = \nabla \times T \tag{2}$$

By using Maxwell's equation which is:

$$\nabla \times H = J = \nabla \times T \tag{3}$$

And Then,

$$\nabla \times (H - T) = 0 \tag{4}$$

And also the vector (H-T) which can be declared as:

$$H = T - \nabla\Omega \tag{5}$$

Note that, Ω is a magnetic scalar potential. And, Since:

$$\nabla \times E = -\frac{\partial B}{\partial t} \tag{6}$$

And then:

$$\nabla \times E = \nabla \times \left[\left(\frac{1}{\sigma}\right)\nabla \times T\right] = -\frac{\partial B}{\partial t} = -\mu_0\mu_r\left(\frac{\partial}{\partial t}\right)(T - \nabla\Omega) = -\mu_0\mu_r\left(\frac{\partial T}{\partial t}\right) - \nabla\left(\frac{\partial \Omega}{\partial t}\right) \tag{7}$$

The final two scalar equations used by Magnet are:

$$\nabla^2 T - \mu\sigma\left(\frac{\partial T}{\partial t}\right) = -\mu\sigma\nabla\left(\frac{\partial \Omega}{\partial t}\right) \tag{8}$$

And

$$\nabla^2 \Omega = 0 \tag{9}$$

The simulation is done between unaligned to full aligned position of rotor. In unaligned position where a stator pole is opposite to the rotor pole, the reluctance of the phase winding has its maximum value which causes the inductance of the phase to be in minimum value. Figure-7 shows the inductance of the phase winding versus rotor position. In fully aligned position where the stator and rotor poles are aligned completely, there is only small air gap between the stator pole and rotor pole which causes the reluctance and the inductance of the phase winding to be minimum and maximum respectively.

The rotor in each simulation is rotated between these two regions. Each position is defined as a problem for the software and at end the parameters in each component like flux, flux path, flux density, losses, forces and torques are obtained. The problems can be solved for different values of phase excitation current.

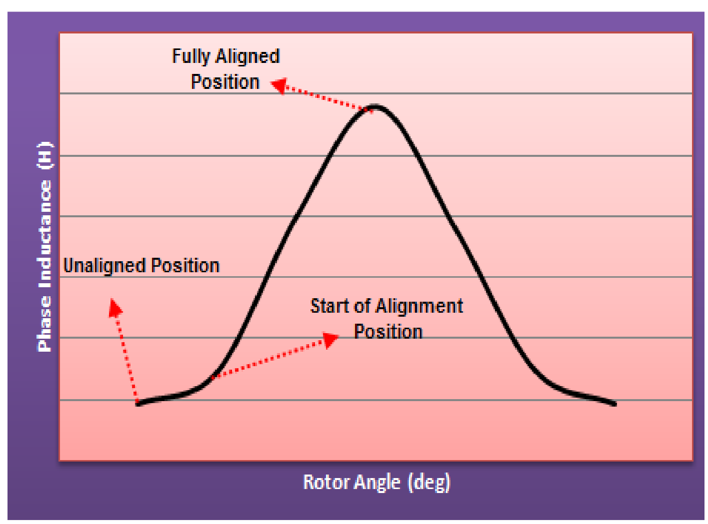

Figure-7
The phase inductance versus rotor position

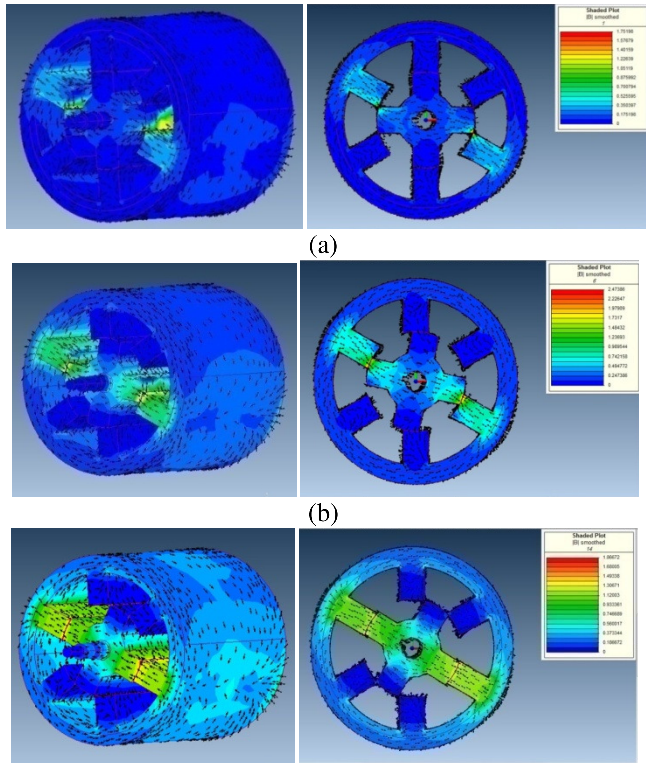

(a)

(b)

(c)

Figure-8
6 by 4 simulation in: a) unaligned, b) half aligned and c) full aligned position

6 by 4 SRM analyses: Figure-8 illustrates the simulation of 6 by 4 SRM in unaligned, half aligned and fully aligned position of rotor. This result is obtained for a phase excitation dc current of 3A and the phase winding of 150 turns. The flux completes its path through the yoke, stator pole, air gap, rotor pole and then another stator pole. As it's observed, the flux density is much higher in the exited pole of the stator in comparison with other poles. Usually the stator pole is thinner than rotor pole in SRMs which causes the stator pole to be in higher value of saturation than rotor poles. The maximum value of flux density is about 1.49 Tesla which is occurred in fully aligned position of rotor.

The simulation is performed for other value of phase excitation dc currents. Flux curve versus rotor position is shown in Figure-9 for different value of currents. The rotor is rotated from unaligned position (-30 deg) to aligned position (0 deg) and again to unaligned position with the next stator pole (30 deg). As it's illustrated the flux has higher value when the phase excitation current is higher. It's starts to increase in the start of alignment position and has its maximum value in fully aligned position.

The generated torque in the rotor component is also obtained in different values of current for the presented 6 by 4 SRM which is shown in Figure-10. As it's illustrated, the torque starts to increase in the start of alignment position and have its maximum value in fully aligned position region and then starts to decrease. Higher value of excitation current increases the value of the generated torque in rotor. The maximum value of torque is about 1.8 N.m. for the phase excitation current of 6 A.

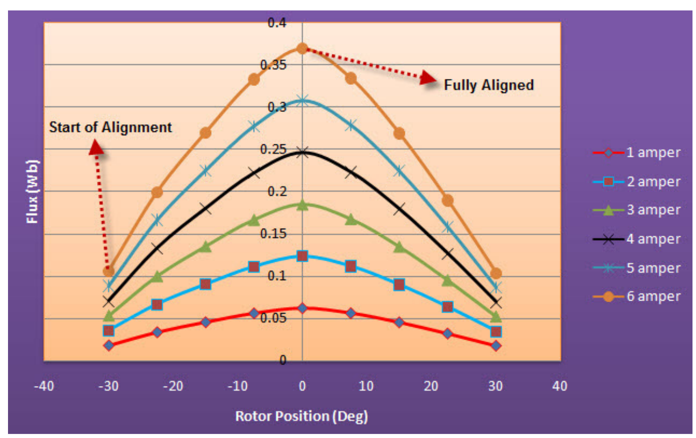

Figure-9
6 by 4 fluxes versus rotor position curve for different value of phase excitation current

Seven-Layer 4 by 4 MSRM Analyses: The field simulation of the 7-layer 4 by 4 MSRM is presented in Figure-11 for unaligned, half aligned and fully aligned position of rotor. As it is shown, three phases are excited in this MSRM. The phase excitation current is 3 A. The maximum value of flux density in fully aligned position of rotor is about 1.43 Tesla.

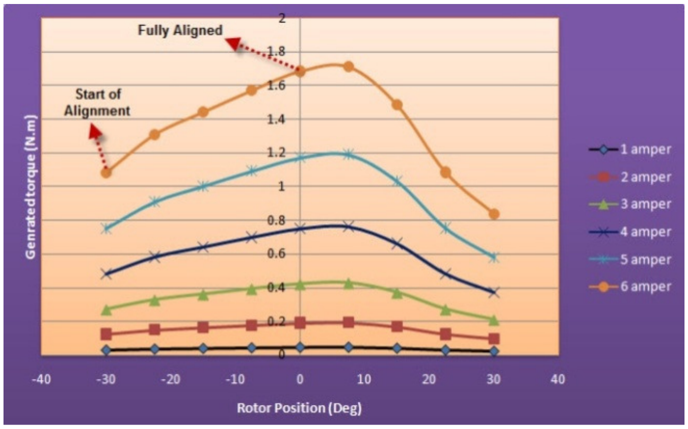

Figure-10
6 by 4 generated torque versus rotor position curve for different value of phase excitation current

The simulation is done for other value of excitation currents. Flux curve of this MSRM versus rotor position is presented in Figure-12 for different value of phase currents. The rotor is rotated from unaligned position (0 deg) to aligned position (12.86 deg). As it's illustrated, the flux starts to increase in the start of alignment position and has its maximum value in fully aligned position.

The generated torque of rotor is depicted in Figure-13 in different position of rotor. As it's illustrated, the torque starts to increase in the start of alignment position and have its maximum value in fully aligned position region and then decreases. The maximum value of torque is about 5.1 N.m. in the phase excitation current of 6 A.

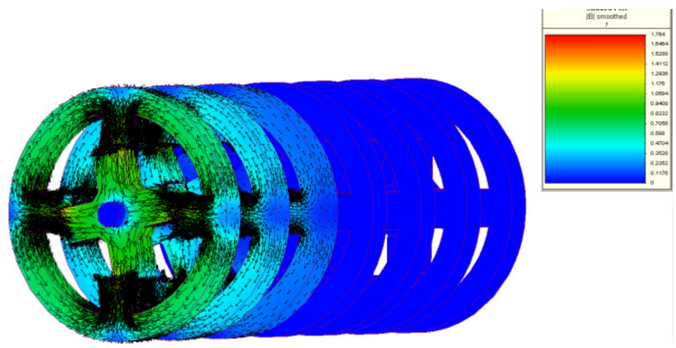

(a)

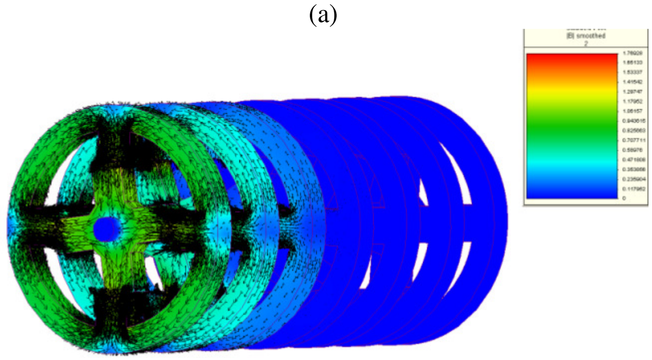

(b)

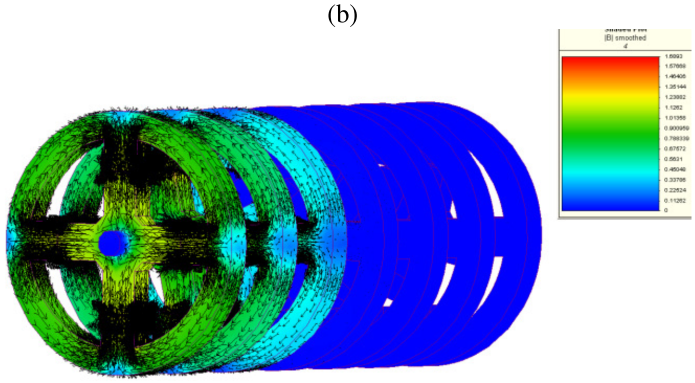

(c)

Figure-11
7-layer 4 by 4 MSRM simulation in: a) unaligned, b) half aligned and c) full aligned position

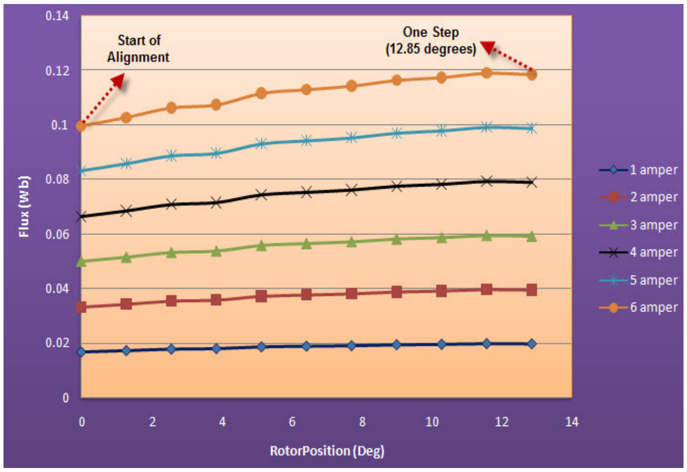

Figure-12
7-layer 4 by 4 MSRM flux versus rotor position curve for different value of phase excitation current

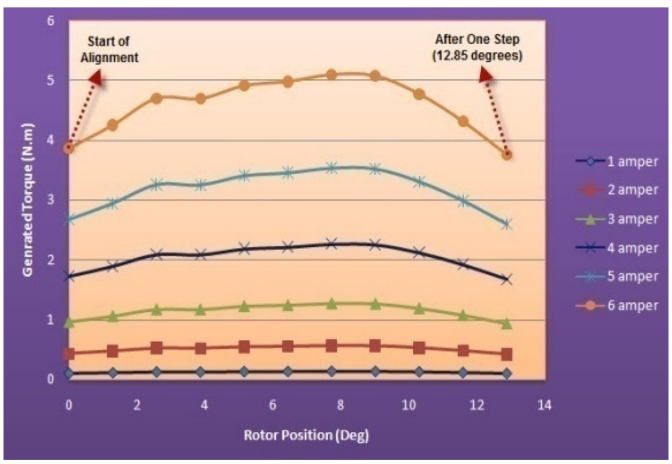

Figure-13
7-layer 4 by 4 MSRM generated torque versus rotor position curve for different value of phase excitation current

Comparing the Simulation Results of The Proposed Motors: The flux values in the flux curves starts to increase in start of alignment position and has its maximum value in fully aligned position of the rotor. The flux of the 6 by 4 SRM at 3 A, is about 0.185 Wb in fully aligned position, is much higher than 7-layer 4 by 4 MSRMs (0.05 Wb in fully aligned position).

The rotor generated torques in these motors were presented for variation of rotor position from unaligned to fully aligned position. For example for the phase excitation current of 6A as it was illustrated, the generated torque in the rotor of the 7-layer 4 by 4 MSRM (=about 5.1 N.m in fully aligned region) is about double of the generated torque of 6 by 4 SRM. The 6 by 4 generated torque value in the same region is about 1.9 N.m. By comparing the torque curves, it can be observed that MSRMs generate more torque in their rotor rather than 6 by 4 conventional SRM. The 7-layer 4 by 4 MSRM has less torque ripple, because three layers are always excited which means the torque is continually generated.

In 7-layer 4 by 4 MSRM the torque is about 3.9 N.m in start of alignment position. It increases to about 5.1 N.m and then decreases to about 3.9 N.m again. The 6 by 4 SRM generates 1.1 N.m torque at first. The value of torque is then increases to about 1.9 N.m and falls down to 0.6 N.m.

Operational Results of the Constructed Srms

The presented 6 by 4 SRM and 7-layer 4 by 4 MSRM are then constructed and tested in laboratory.

Operational Results of the 6 by 4 SRM: The operational results of the 6 by 4 three-phase SRM are as follows. Three opto-counter sensors and a plate are coupled on the motor shaft and the motor is tested. The supply voltage of the motor is 60 volts and the driver circuit which is an asymmetric bridge converter uses 12 volts power supply.

The motor is tested under different load and speed conditions and its operational results are obtained.

The command pulses of three phases which are obtained from the opto-counters are shown in Figure-14.

Figure-15 shows the generated torque of the motor versus the operational speed. In the speed of about 3200 rpm, the minimum value of torque which is about 0.039 N.m is generated. In the speed of about 461 rpm, the maximum generated torque of about 2.35 N.m is produced.

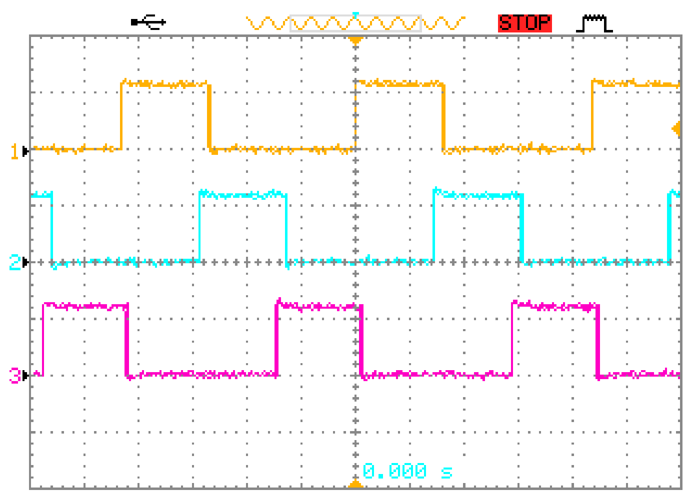

Figure-15
Command pulses of three phases

The motor current versus generated torque is illustrated in Figure 16. In the maximum speed where the minimum value of torque is generated (0.039 N.m), the motor current is about 1.59 A. In the minimum speed of the motor where the maximum torque is generated (2.35 N.m), the motor current is about 5.47A.

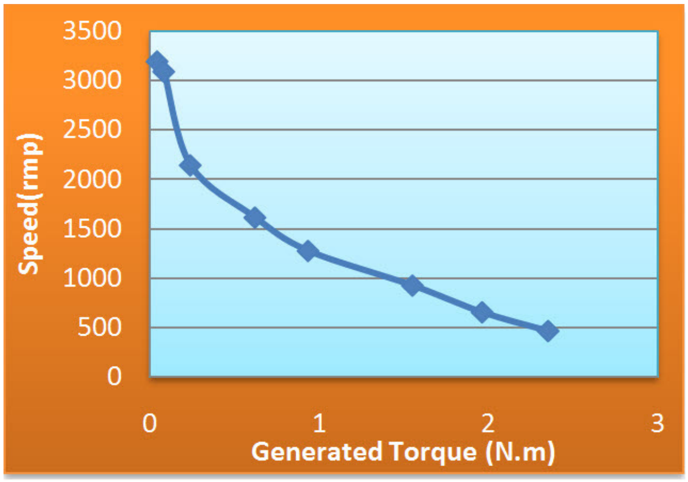

Figure-16
Torque versus speed in 6 by 4 SRM

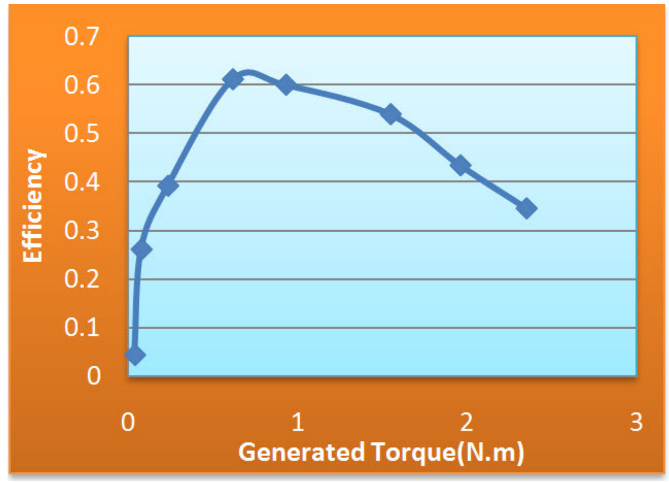

Figure-18
Efficiency versus torque in 6 by 4 SRM

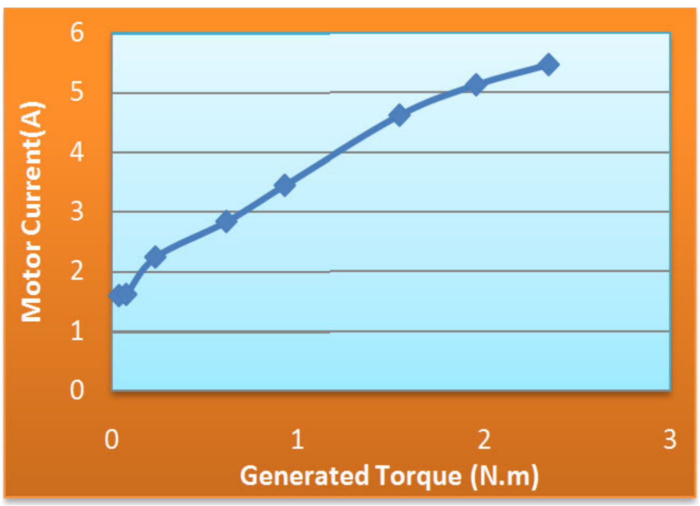

Figure-17
Current versus torque in 6 by 4 SRM

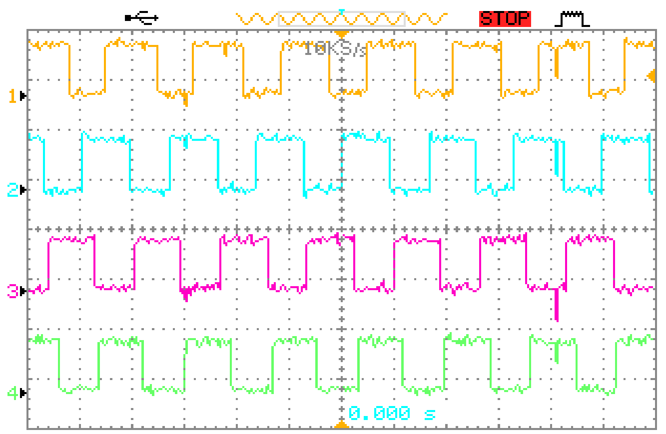

Figure-19
Command pulses of four phases in 7-layer MSRM

The motor efficiency versus generated torque is shown in Figure 17. In the minimum value of torque (0.039 N.m), the motor efficiency is about 4.4%. In the maximum generated torque (2.35 N.m), the motor has the efficiency of about 34.5%. The maximum value of efficiency is about 61% which is in the speed of about 1611 rpm and the generated torque of about 0.617 N.m.

Operational Results of Seven-layer 4 by 4 MSRM: Seven opto-counter sensors and a plate are coupled on the motor shaft and the motor is tested. The supply voltage of the motor is 60 volts and the driver circuit which is an asymmetric bridge converter uses 12 volts power supply.

The motor is tested under different load and speed conditions and its operational results are obtained.

The command pulses of four phases (four layers) which are obtained from the opto-counters are shown in Figure-18.

Figure-19 shows the generated torque of the motor versus the operational speed. In the speed of about 3300 rpm, the minimum value of torque which is about 0.0391 N.m is generated. In the speed of about 216 rpm, the maximum generated torque of about 5.3 N.m is produced.

The motor current versus generated torque is illustrated in Figure 20. In the maximum speed where the minimum value of torque is generated (0.0391N.m), the motor current is about 2.13 A. In the minimum speed of the motor where the maximum torque is generated (5.3 N.m), the motor current is about 8.24A.

The motor efficiency versus generated torque is shown in Figure 21. In the minimum value of torque (0.0391 N.m), the motor efficiency is about 10.7%. In the maximum generated torque (5.3 N.m), the motor has the efficiency of about 24.2%. The maximum value of efficiency is about 72.2% which is in the speed of about 722 rpm and the generated torque of about 3.23 N.m.

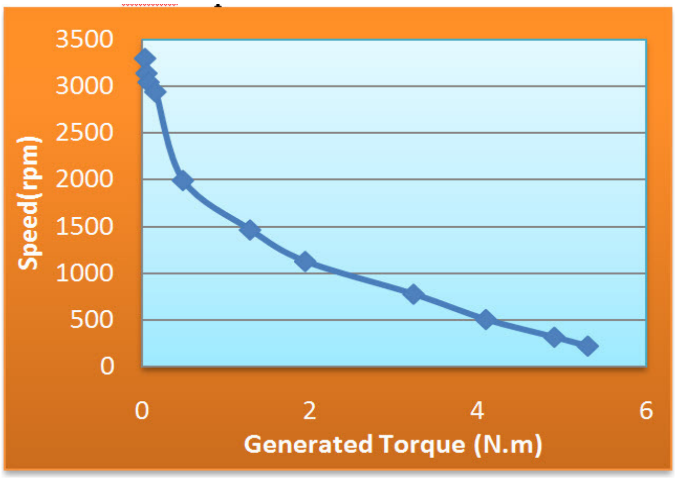

Figure-20
Torque versus speed in 7-layer MSRM

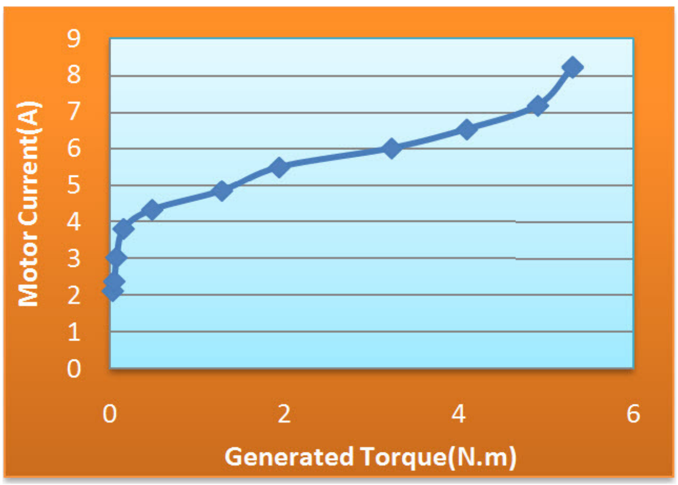

Figure-21
Current versus torque in 7-layer MSRM

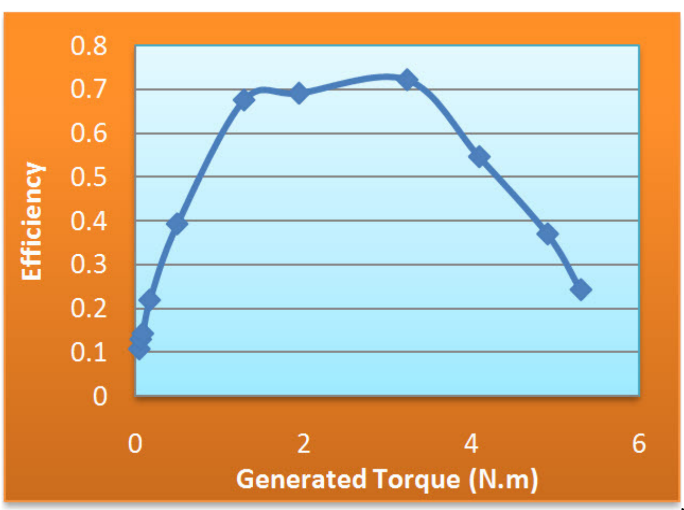

Figure-22
Efficiency versus torque in 7-layer MSRM

Comparing the Operational Results of The Proposed Motors: The operational results of the presented SRMs are compared in this section. The speed-torque specifications of the these SRMs were illustrated in Figure-9, 12 which show that by increasing the number of independent layers of the SRM (with a same iron volume), the generated torque of the motor increases. It was also shown that the torque ripple is reduced by increasing the number of layers. The maximum generated torque of the 6 by 4 SRM is about 2.35 N.min the speed of about 461 rpm. In 7-layer 4 by 4 MSRM, the maximum generated torque is about 5.3 N.m in the speed of about 216 rpm.

As shown in the speed-efficiency specifications of the SRMs by increasing the number of independent layers of the SRM (with a same iron volume), the efficiency of the motor increases. The maximum efficiency of the presented 6 by 4 SRM which is obtained in laboratory is about 61% that is obtained in the speed of about 1611 rpm and the generated torque of about 0.617 N.m. The maximum value of efficiency obtained from the 7-layer 4 by 4 MSRM is about 72.2% which is in the speed of about 722 rpm and the generated torque of about 3.23 N.m.

Conclusion

This paper presented the characteristics of two different types of SRM with the same iron volume. They were 6 by 4 SRM and 7-layer 4 by 4 MSRM. The 6 by 4 SRM which was a three phase motor, had six stator and four rotor salient poles. The MSRMs had four stator and four rotor salient poles in each layer.

These motors were numerically analyzed at first and their electromagnetic parameters were obtained by FEM analysis in Magnet software which is a powerful 3D simulator in electromagnetic problems. The different positions of the rotor were determined as the problems of the simulations. Then the rotor was rotated from unaligned to fully aligned position and the motor parameters like flux, flux density, electromagnetic force, torque etc were obtained for each problem of the motor. The motors were then fabricated and tested in laboratory under different load conditions.

In the 7-layer MSRM, three layers were switched on each time. More than one layer excitation at a moment caused the MSRMs produced more torque with less torque ripple rather than custom 6 by 4 SRM. The different parameters of motors were illustrated in figures which were in close agreement with the experimental results obtained in laboratory. The torque of the rotor in MSRMs was about double of the 6 by 4 produced torque. The 6 by 4 SRM had the maximum torque of about 2.35 N.m while the presented 7-layer 4 by 4 MSRM had the maximum torque of about 5.3 N.m. The efficiency of the MSRMs were also higher than custom SRM. The maximum efficiency of the presented custom 6 by 4 SRM was about 61% while the presented 7-layer 4 by 4 MSRM had the efficiency of about 72.2%.

References

1 Miller T.J. (1988), Switch Reluctance Motor Drive, Ventura, CA; Intertec Communications Inc.

2 Vijayakumar K., Karthikeyan R., Paramasivam S., Arumugam R. and Srinivas K.N. (2008). Switched Reluctance Motor Modeling, Design, Simulation, and Analysis: A Comprehensive Review, IEEE Transactions on Magnetics, 44(12), 4605-4617.

3 Krishnan R. (2001). Switched Reluctance Motor Drives, Modeling, Simulation, Analysis, Design and Applications, CRC Press.

4 Krishnan R. (2001). Electric Motor Drives, Modeling, Analysis and Control, Printice Hall.

5 Torkaman H., Afjei E. and Toulabi M.S. (2012). New Double-Layer-per-Phase Isolated Switched Reluctance Motor: Concept, Numerical Analysis, and Experimental Confirmation, IEEE Transactions on Industrial Electronics, 59(2), 830-838.

6 Ding W., Liang D. and Tang R. (2011). A fast nonlinear variable structure equivalent magnetic circuit modeling for dual-channel switched reluctance machine, IEEE Transactions on Energy Conversion and Management, 52(1), 308-320.

7 Wang H., Lee D.H. and Park T.H. et al. (2011). Hybrid stator-pole switched reluctance motor to improve radial force for bearingless application, IEEE Transactions on Energy Conversion and Management, 52(2), 1371-1376.

8 Daldaban F. and Ustkoyuncu N. (2011). A novel linear switched reluctance motor for railway transportation systems, IEEE Transactions on Energy Conversion and Management, 52(3), 465-469.

9 Daldaban F. and Ustkoyuncu N. (2006). A new double sided linear switched reluctance motor with low cost, IEEE Transactions on Energy Conversion and Management, 47(18-19), 2983-2990.

10 Daldaban F. and Ustkoyuncu N. (2008). Multi-layer switched reluctance motor to reduce torque ripple, IEEE Transactions on Energy Conversion and Management, 49(5), 974-979.

11 Daldaban F. and Ustkoyuncu N. (2007). New disc type switched reluctance motor for high torque density, IEEE Transactions on Energy Conversion and Management, 48(8), 2424-2431.

12 Lee C. and Krishnan R. (2009). New Designs of a Two-Phase E-Core Switched Reluctance Machine by Optimizing the Magnetic Structure for a Specific Application: Concept, Design, and Analysis, IEEE Transactions on Industry Applications, 45(5), 1804–1814.

13 Torkaman H. and Afjei E. (2012). Comparison of Three Novel Types of Two- Phase Switched Reluctance Motors Using Finite Element Method, Progress in Electromagnetics Research (PIER), 125(151-164).

14 Oh S.G. and Krishnan R. (2007). Two-phase SRM with flux-reversalfree stator: concept, analysis, design, and experimental verification, IEEE Transactions on Industry Applications, 43(5), 1247-1257.

15 Oyama J., Higuchi T. and Abe et al. T. (2004). Characteristics of a hybrid-type switched reluctance motor with salient pole stator," Electrical Engineering in Japan, 147(3), 72–79.

16 Chen H. and Gu J.J. (2010). Implementation of the Three-Phase Switched Reluctance Machine System for Motors and Generators, IEEE/ASME Transactions on Mechatronics, 15(3), 421-432.

17 Takahashi et all. (2006). Characteristics of 8/6 Switched Reluctance Generator Excited by Suppression Resistor Converter, IEEE Transactions on Magnetics, 42(10), 3458-3460.

18 Radimov N., Ben-Hail N. and Rabinovici R. (2006). Switched Reluctance Machines as Three-Phase AC Autonomous Generator, IEEE Transactions on Magnetics, 42(11), 3760-3764.

19 Toulabi M.S., Torkaman H. and Afjei E. (2012). Experimental and Numerical Comparison between the Output Voltages of Two Novel Switched Reluctance Generators, COMPEL: The International Journal for Computation and Mathematics in Electrical and Electronic Engineering, 31(2), 401-423.

20 Afjei E. and Toliyat H.A. (2002). A novel multilayer switched reluctance motor", IEEE Transaction on Energy Conversion, 17(2), 217–221.

21 Magnet (2006). CAD Package: User Manual, Infolytica Corporation Ltd., Montreal, Canada.